View Article Online
DOI: 10.1039/C7CP08406D

Journal Name

ARTICLE

Polydopamine films changes their physiochemical and antimicrobial properties with change in reaction conditions.

Received 00th January 20xx,
Accepted 00th January 20xx

DOI: 10.1039/x0xx00000x

www.rsc.org/

Khushbu Patel[#a], Nimisha Singh[#a], Jyoti Yadav [a], Jyotsna M. Nayak [a], Suban K Sahoo [a], Jeevan Lata[b], Duni Chand[b], Shashank Kumar [c] and Rajender Kumar[*a].

The morphology and physiochemical properties of polydopamine is not totally inherent and undergo changes with reaction conditions like choice of solvent used for polymerization. The polymerisation of dopamine to polydopamine carried out in different solvents like sodium hydroxide, sodium bicarbonate, PBS and Tris reveals exceptionally different morphological and physiochemical features with each solvent. Additionally, the different physiochemical characteristics and morphologies bestow the polymer films with different extent of antimicrobial activity. Moreover, the findings, supported by chemical evidences from X-ray photoelectron spectroscopy reveal that higher antibacterial properties were obtained against E.*coli* and S.*aureus* with polydopamine films prepared in Tris and NaOH solvent induced polymerization. Antibacterial activity observed in saline was found to be higher than PBS medium for both E.coli and S. aureus. The higher antibacterial properties of polydopamine films prepared in Tris and NaOH solvents were attributed to the covalent incorporation of –OH groups on the surface provided by nucleophilic Tris and NaOH solvents during polymerisation process. The distinct physiochemical and morphological changes were supported by the contact angle, FE-SEM, EDAX, AFM, and XPS analysis. The present finding provides an insight in to the different chemistry, morphology and properties of the designed polydopamine films with controlled antibacterial/antifouling properties. Additionally, new insight in to the mechanism of formation, physiochemical changes in morphology and properties of polydopamine coatings were revealed.

Introduction

Biofouling is a vital phenomenon responsible for the host of diseases and infections.[1-3] Particularly vulnerable are the water treatment membranes and medical implant devices which are prone to biofouling once in contact with the cellular/biological environment.[4, 5] An interesting alternate is to develop biofouling resistant antimicrobial coatings on the medical implants.[6, 3] Several polymer coatings have been developed for the implants with increasing antibacterial properties.[7-10]

Polydopamine surfaces have proved to be of versatile utility on account of their strong antimicrobial nature, adhesion and antibiofouling properties.[11-13] The polydopamine has strong adhesive properties and can adhere to almost any surface ranging from, mica, metals, polymers etc.[14] Messersmith et.al, inspired by the mussel adhesive proteins, reported the polymerization of dopamine under mild oxidative conditions in to the polydopamine layers.[15] On basis of the findings of Messermith et.al several investigations and reports have appeared highlighting the huge potential of polydopamine layers in antimicrobial/ antifouling surface designs.[16, 17] In addition to native polydopamine layers several functional groups have been incorporated on to the surface of polydopamine layers for efficient antimicrobial/antibiofouling properties.[3, 13, 18-22] PDA layers have been reported to be coated on the AgNPs[23-26] and stainless steel[27, 28] for the strong antifouling and anticorrosive properties. Also, it has been reported that polydopamine helps in the wound healing and show high biocompatibility and non-cytotoxicity both in vitro and in vivo.[29-31]

However, the structure of the polydopamine is very complex and full structure and mechanism of its formation is not still established conclusively.[32] Although, several structures and mechanistic pathways has been proposed[32, 33] but no clear mechanism of its formation and account of its antibacterial properties has been reported. Polydopamine formations have been extensively studied [33-35] but all reports are focussed on the polydopamine formation for specific applications and don't involve the study of solvents effect on physiochemical properties and morphology of polydopamine films probably due to the different aspects of study. *D'Ischia et al.,* studied the effect of Tris buffer on the formation of polydopamine nanoaprticles.[36,37] However, the solution chemistry and

[a] *Department of Applied Chemistry, S.V. National Institute of Technology Surat-395007 Gujarat, India.*
[b] *Department of Biotechnology, Himachal Pradesh University, Summerhill, Shimla-05.*
[c] *Department of Biochemistry and Microbial Sciences, Central University of Punjab, Bathinda, India-151001*
† Footnotes relating to the title and/or authors should appear here.
Electronic Supplementary Information (ESI) available: See DOI: 10.1039/x0xx00000x

View Article Online
DOI: 10.1039/C7CP08406D

morphology and physiochemical properties of films prepared on surface may differ to a significant extant. Thus, the choice of reaction conditions like solvents can have interesting effects on surface morphology and ensuing properties of the polymer layers.[38]

In order to decipher these vital surface phenomenons and their dependence on reaction conditions we studied the effect of four solvents for PDA film formation and their subsequent effect on the morphology of the PDA films. Since the film morphology and surface chemistry can have profound effect on antibacterial properties,[38] therefore, we also investigated the effect of solvents controlled morphology and chemistry on accompanying antibacterial properties.

Thus, in this report we have studied the coatings of polydopamine on the PET surfaces under four different solvent conditions and tried to establish the structural and morphological changes in prepared films using XPS, AFM, FE-SEM, ATR-FTIR etc.

We choose the PET films as the base substrate because these are one of the most used films in articles ranging from food, beverages, and water bottle etc.[39, 40] and thus can be improved upon by PDA coatings for their antifouling efficacy. We also checked the PDA coatings prepared in different solvents for their antimicrobial properties using gram positive and gram negative bacteria. To our amazement, the PDA layers prepared with different solvents not only show different structural, chemical and morphological features but also different extent of antibacterial activities.

A comparison with all solvents used in polydopamine formations reveals a direct correlation between nucleophilic group incorporation in to the polydopamine surfaces during polymerisation process and ensuing antibacterial properties, with higher antibacterial activities for PDA layers prepared in Tris and Na-OH layers in both saline and PBS medium. The extent of antibacterial properties were well justified from experimental evidences. Thus, in this report we have successfully decipher an important aspect of PDA coating which would be beneficial in tuning the antibacterial propensity of PDA surfaces in particular and other polymeric surfaces in general and would help in improving the antibacterial features of commonly used films such as PET making them more effective to prevent microbial infections.

Furthermore, these findings helps in understanding the mechanism of polymerization and solvent induced changes in the morphology and chemistry of the polydopamine films which significantly influences the antimicrobial behaviour of PDA layers on surface and would be beneficial to design biocompatible antifouling coatings.

To the best of our knowledge this is first report which describes in detail the effect of solvent conditions on polydopamine film formations on PET surfaces and resulting antibacterial properties.

Result and Discussion

The schematic representation of PDA coatings prepared on PET films in different solvents is shown in Scheme-1. It's to be noted that in scheme-1 the wavy bonds connecting ring to the surfaces are for illustration only and doesn't represent the true covalent bond since molecular mechanism of binding of polydopamine to surfaces is not known. [32]

The polydopamine films were prepared by polymerisation of

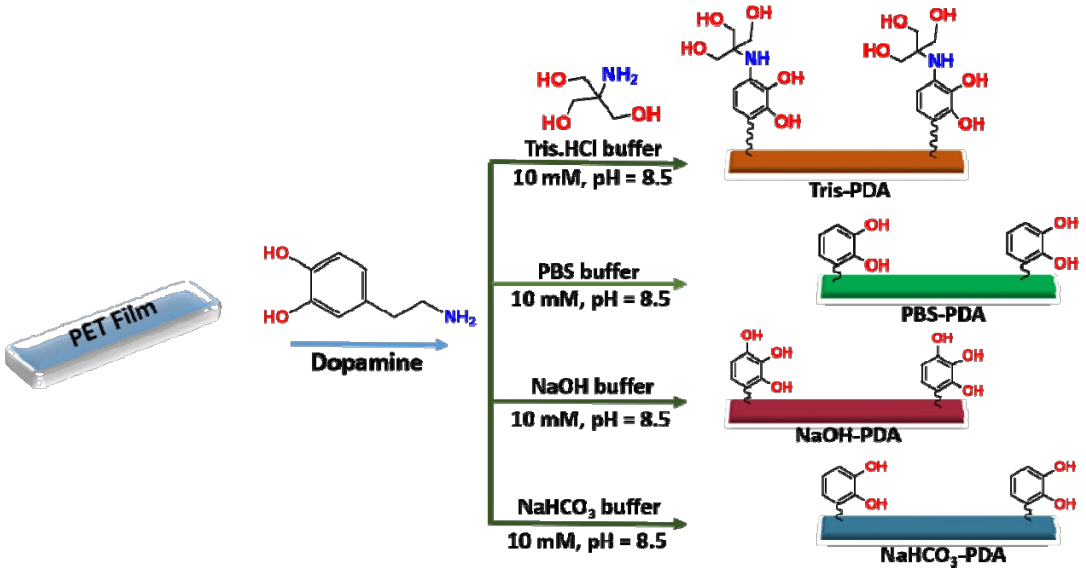

Scheme 1: Preparation of polydopamine coatings on PET films using dopamine polymerization in Tris, PBS, NaOH and $NaHCO_3$ solvents under oxidative conditions with shaking for 24 hours.

View Article Online
DOI: 10.1039/C7CP08406D

dopamine using four different solvents viz. Tris, PBS, NaOH and $NaHCO_3$ under similar pH (8.5) and oxidative conditions. The four different buffers were selected for present study as they are the most common buffers reported for the polydopamine formation in literature and may have different effect on the polydopamine morphology and chemistry. After successful PDA coatings on PET films the wettability of the surfaces was measured. Wettability plays substantial role in controlling adhesive and antimicrobial properties of the surfaces.[41, 42] The images of contact angle measured on the PDA coatings prepared on PET surfaces after 24 hours is shown in Fig. 1.

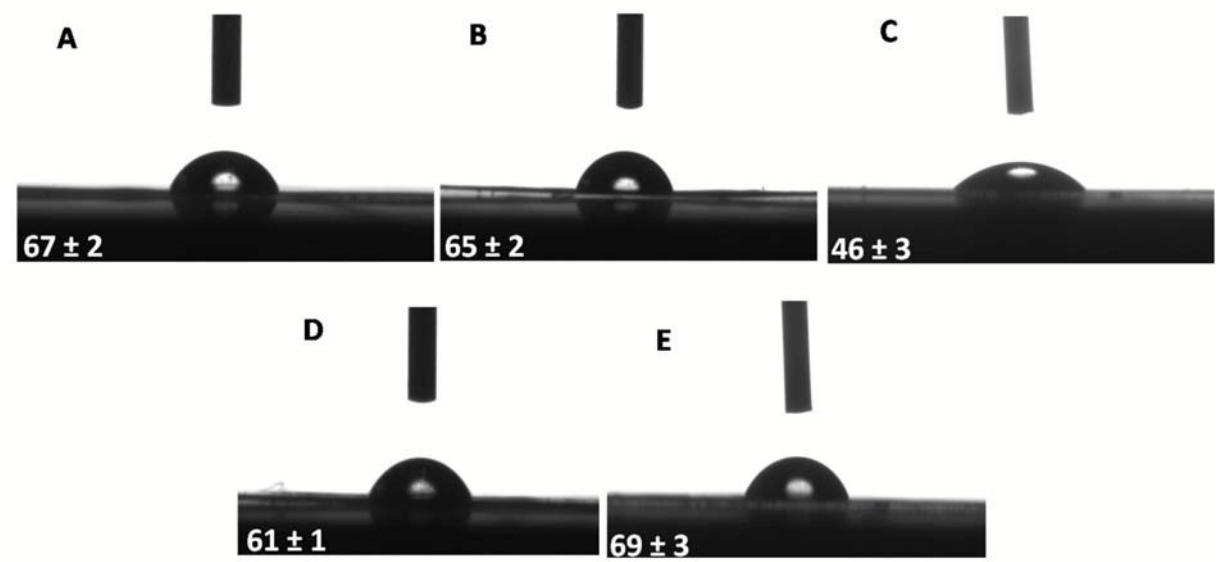

Figure 1: Contact angle of (A) Uncoated PET film (B) PDA coated PET film prepared in Tris Solvent, (C) PDA coated PET film using PBS Solvent, (D) PDA coated PET film using NaOH Solvent and (E) PDA coated PET film using $NaHCO_3$.

The PDA coating formed in PBS solvent (PBS-PDA) shows maximum wettability, while the lowest wettability (Fig. 1) was shown by PDA coatings prepared in $NaHCO_3$ solvent (NaHc-PDA). On the other hand the PDA layers prepared in Tris solvent (Tris-PDA) shows the contact angle of 65° which is almost near to the uncoated PET films. This observation could be explained on the basis of the covalent incorporation of Tris in to PDA layers.[36, 37]

The Tris solvent contains three hydroxyl groups per molecule and as such should have increased the wettability, however in addition to the –OH groups it also adds additional unit of $–CH_2$ per –OH group which may be the reason for the lower wettability of the Tris-PDA as hydrocarbon unit leads to decrease in wetability.[43] It has been reported that contact angle though a surface property is strongly affected by the characteristics such as topography and morphology in addition to underlying functional groups.[43-45] So in present case we believe that –-CH_2 groups coming with Tris also contributes towards increase in contact angle and hence we didn't see increase in wettability in Tris-PDA. The early termination of polymerization process in presence of Tris may also contribute towards higher contact angle for Tris-PDA.[36, 37] Additionally, the Tris-PDA is capable of extensive intramolecular hydrogen bonding in addition to intermolecular hydrogen bonding (Fig. 2) which may also contributes towards higher contact angle of Tris-PDA.

.

View Article Online
DOI: 10.1039/C7CP08406D
ARTICLE Journal Name

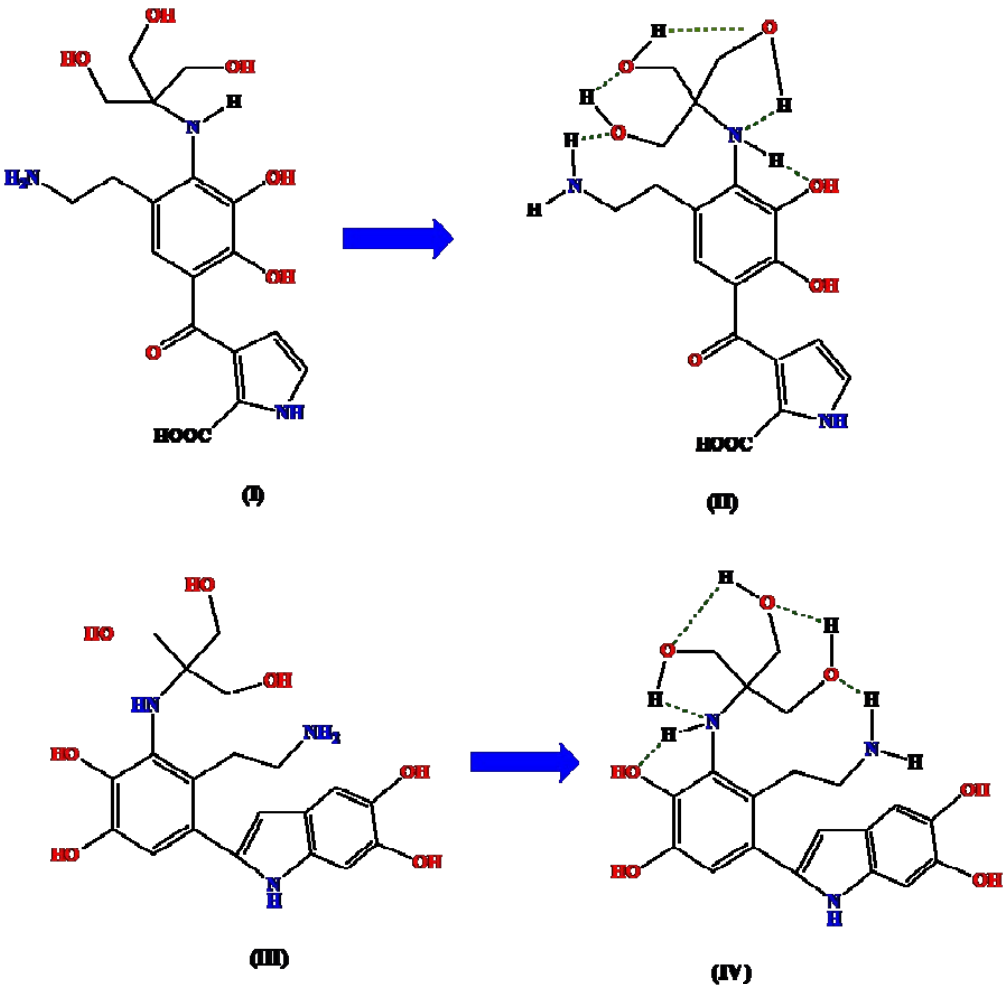

Figure 2: Tris incorporated PDA (I & III) showing intramolecular hydrogen Bonding (II &IV). Structure I and III were taken from Reference D'Ischia et al., Langmuir 2014, 30 (32), 9811-8.

View Article Online
DOI: 10.1039/C7CP08406D

The contact angle of various surfaces with respect to the polymerization time (Fig. 3) shows that compared to uncoated PET films, contact angle of PBS-PDA and Tris-PDA first increases during initial one hour of polymerization and then decreases up to six hours and thereafter rises again from nine to twenty four hours. However, for NaOH-PDA the contact angle increases after initial one hour and shows further small increase with time till 24 hours. In case of NaHc-PDA there was sharp decrease in the contact angle after one hour and then increases from 3 to 6 hours, becoming steady till 9 hours. All coatings except Tris-PDA shows decrease in contact angle from 9 to 18 hours which again rises from 18 to 24 hours. It was observed that in all time groups the wettability of PBS-PDA coatings was highest and the NaHc-PDA shows the lowest wettability.

The FEG-SEM analysis of the PDA films shows distinct morphological features with each solvent (Fig. 4) The PBS-PDA and Tris-PDA shows aggregated layers on the surface where several particles appears to form closely adhered layers (Fig. 4 D &E). However the Na-PDA and NaHc-PDA shows loosely held distinct particles of PDA spread over the whole surface.

The particle size distribution of SEM images shows that Na-PDA and NaHc-PDA have smaller particle size while the PBS-PDA and Tris-PDA have larger particle size distribution on account of aggregation (Fig. 5). The Tris-PDA shows the largest particle size because of the aggregation and covalent incorporation of Tris Solvent in to the PDA layers. Moreover, the presence of extensive hydrogen bonding due to the hydroxyl groups of Tris incorporated PDA layers may result in strong adherence of the Tris-PDA particles.

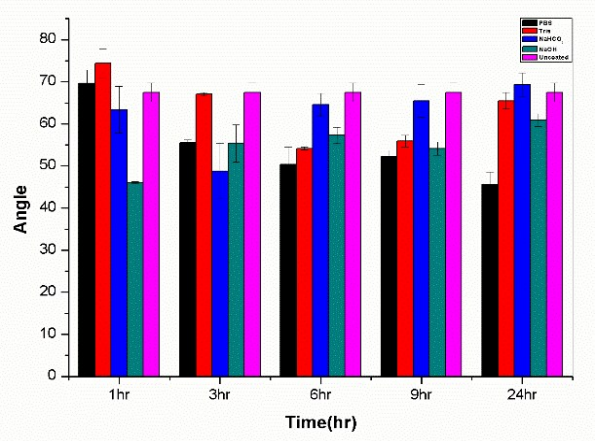

Figure 3: Contact angle of PDA coatings on PET films prepared in different solvents as function of time.

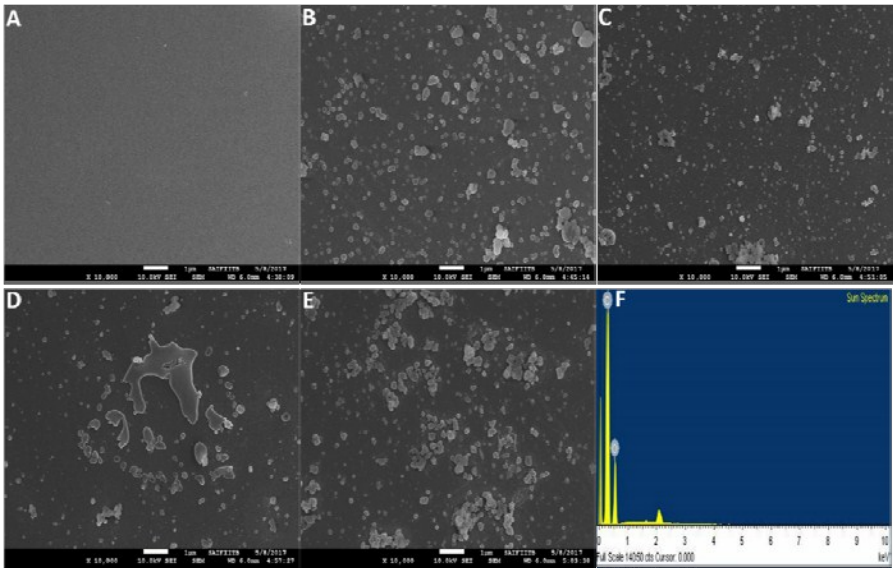

Figure 4: FEG-SEM images (A) Uncoated PET, (B) NaHc-PDA, (C) NaOH-PDA, (D) PBS-PDA (E) Tris-PDA and (F) EDS Spectrum of uncoated PET film.

View Article Online
DOI: 10.1039/C7CP08406D
ARTICLE Journal Name

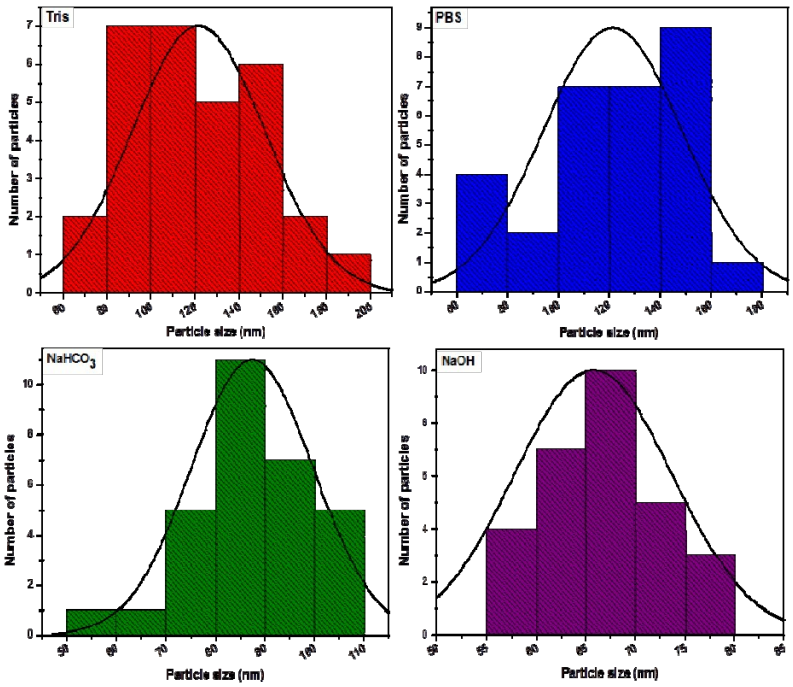

Figure 5: Particle size distribution calculated from FEG-SEM images for Tris-PDA, PBS-PDA, NaHc-PDA and NaOH-PDA.

The high magnification FEG-SEM images as shown in Fig. S1 shows that for NaOH-PDA the particles are scattered over the whole surface with cauliflower like outgrowth on the surface. In the PBS-PDA (Fig. S2) on the other hand, the PDA particles seem to be aggregated to form a continuum of layers which appeared as thick patches on the surface.

Similarly for Tris-PDA the growth on surface was not continues and shows highly aggregated layer type structure as shown in Fig. S3. This behaviour is suggestive that the PBS and Tris assisted polymerization leads to self-adhering of the PDA particles to form the aggregated layers while the NaOH and $NaHCO_3$ (Fig. S4) have limited effect on adherence of the PDA particles forming distinct spherical particles of PDA on PET surfaces. The chemical

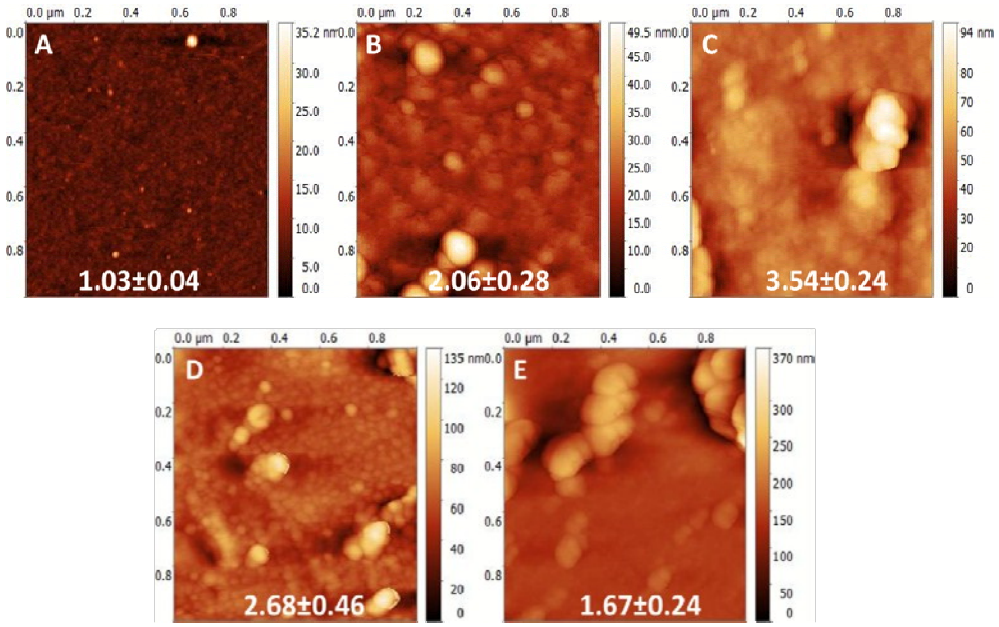

Figure 6: AFM images (A) Uncoated PET film, (B) Tris-PDA, (C) PBS-PDA, (D) NaHc-PDA and (E) NaOH-PDA.

View Article Online
DOI: 10.1039/C7CP08406D

constitution of the PDA particles evaluated using EDS mapping is shown in (Fig. S1-S4) at the base of SEM images of different PDA layers. The EDAX analysis indicates the presence of N in addition to the C and O in the PDA layers. The absence of N in the uncoated PET films and its presence on PDA coated PET films confirms the formation of PDA coatings.

The NaHc-PDA shows the distinct spherical PDA particles on surface with uniform distribution on the surface of PET (Fig. S4). Thus FE-SEM clearly shows the distinct morphological changes in the PDA layers prepared using different types of solvent.

Further morphological evidence and surface roughness was determined by AFM. The AFM images of the PDA layers prepared in different solvents on PET surfaces (Fig. 6) confirms that different solvents leads to the different topographical features of PDA coatings.

Compared to uncoated PET films the topography was significantly different for PDA coatings as shown in Fig. 6. Moreover, among the different PDA coatings the surface morphology was significantly different which establishes the role of solvents in controlling the morphological features of PDA layers. The PDA coating of PET leads to the increase in the roughness (RMS) values as shown in Fig. 6. The maximum RMS roughness was observed for the NaOH-PDA followed by PBS-PDA. The roughness value of the $NaHCO_3$ and Tris was least. This roughness pattern was due to the fact that Tris-PDA hinders the complete polymerization of dopamine to polydopamine on account of its binding with electrophilic quinone moieties which devoid the polymerization mixture of required quinones.[36, 37]

The ATR-FTIR reveals (Fig. 7) that all type of PDA coatings prepared using different solvents shows same type of the functionalities. The characteristic peaks in the region at 3700-3400 cm^{-1} are because of the N-H and O-H stretching vibrations. The intense peak in the region of 1721 cm^{-1} is because of the C=O of the Quinone group.[35] The other characteristic peaks present in the PDA coatings were at 1603 cm^{-1} and 1512 cm^{-1} which are characteristic of C=C of aromatic system and C=N of indole amine.[35] Another peak at 1314 cm^{-1} was because of the C-N stretching of the indole ring. Thus, the IR analysis confirms the formation and chemical functionalities present in the coating. The ATR-FTIR spectra of different PDA coatings obtained at different time interval during the polymerization process is shown in Fig. 9B which indicates virtually no chemical difference in functionalities.

Further, the chemical composition of the PDA coatings (top 10 nm) was evaluated using XPS which give precise and highly sensitive information of the top 10 nm layer. Since the XPS cannot penetrate up to the PET through PDA coatings the information about elemental and surface composition is highly specific.[46]

The elemental composition obtained from XPS analysis for different solvent coated PDA films is shown in the Table 1. The maximum N content was found to be in the Tris-PDA. The N/C ratio was highest for the Tris–PDA which was because of the covalent incorporation of the Tris moieties in to the PDA layers.[37, 47] Hence it is well justified that Tris-PDA involves significant contribution from the covalent incorporation of Tris in to PDA coatings.

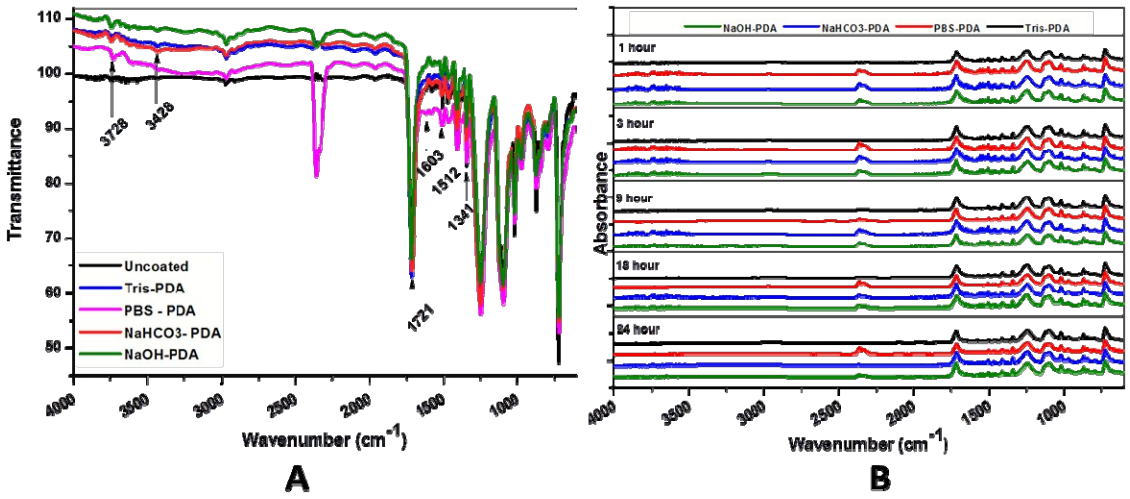

Figure 7: FTIR spectra of PDA coatings on the PET films prepared using different solvents (A) After 24 Hours of coating & (B) at different time interval range from 1-24 hours.

View Article Online
DOI: 10.1039/C7CP08406D

Table 1 : XPS elemental percentage of PDA coated PET films prepared in different solvents.

Samples	Atomic Percentage			N/C ratio
	C	N	O	N/C
Tris	75.49	6.54	17.97	0.1
PBS	82.94	2.49	14.57	0.03
NaOH	79.78	3.21	17.01	0.04
$NaHCO_3$	75.21	2.96	21.83	0.04

The XPS survey scans (Fig.8) shows that all the PDA coated films (Fig. 8 B-E) have the peak for nitrogen in the B.E range of 399-400 eV. However, the uncoated PET film doesn't show the peak for nitrogen (Fig. 8 A). Compared to the uncoated films the peak for B.E of carbon was also shifted to higher binding energy upon coating with PDA layers.

The high resolution deconvoluted XPS spectra of C 1 s peaks for PDA coated PET and uncoated PET films (Fig. 9 I) shows that NaHc-PDA has three types of carbon at B.E of 282.7 eV for C-NH_2 bonds, 284.4 eV for C-O/C-N and 286.5 eV for C=O bond. The area percentage as shown in inset shows that percentage of C=O was minimum in the Tris-PDA and NaOH-PDA. This can be supported by the argument that Tris being covalently bonded to the quinone groups of the PDA coatings[37, 47] decreases the percentage of C=O compared to PBS and

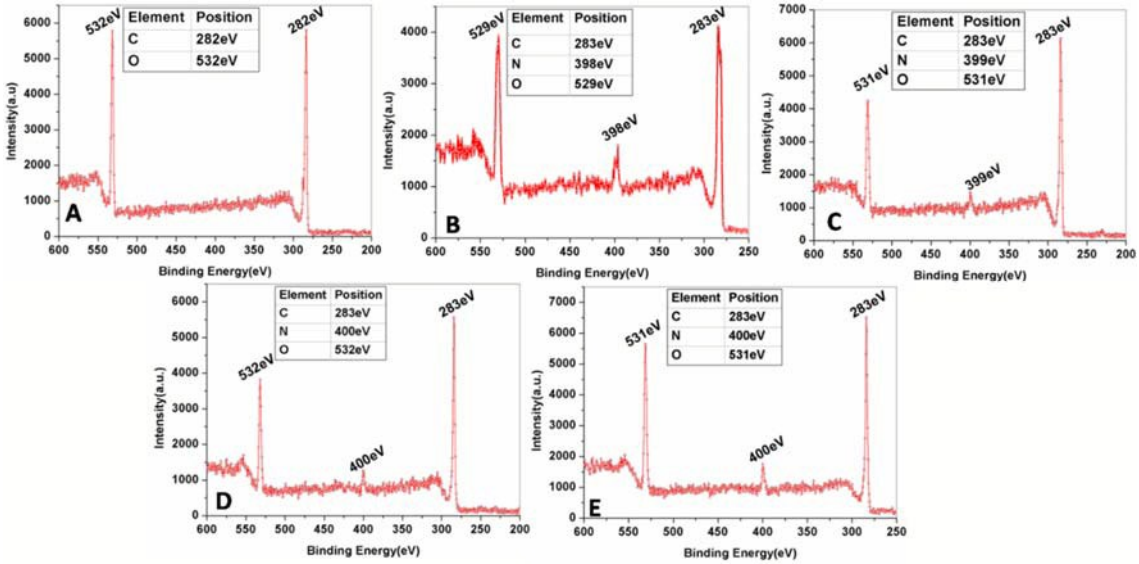

Figure 8: XPS-Survey scan of (A) Uncoated PET films, (B) Tris-PDA (C) PBS-PDA, (D) Na-PDA and (E) NaHc-PDA.

$NaHCO_3$. The same argument can be forwarded for the NaOH-PDA also since OH is a highly nucleophilic species with strong tendency to attack the C=O present in PDA coatings.

The N 1s deconvoluted spectra of the PDA coatings shows three types of the peaks; primary amine (RNH_2), secondary ring amine (R-NH-R) and a tertiary nitrogen (=N-R) as part of ring with BE shown in inset of respective figures. The highest percentage of tertiary nitrogen (=N-R, 27.58%) was found in the Tris-PDA as shown in the inset of Fig. 9 IIA. While for other PDA coatings the difference was significantly higher. This can be explained on the basis of covalent binding of the Tris nitrogen with the quinone groups in the PDA layers[37, 47] which results in increase in the percentage of =N-R species in Tris-PDA. Moreover all the PDA surfaces shows shift in the B.E of various N species depending upon the type of solvent used which clearly establish a distinct chemical process or mechanism operating in each case.

View Article Online
DOI: 10.1039/C7CP08406D

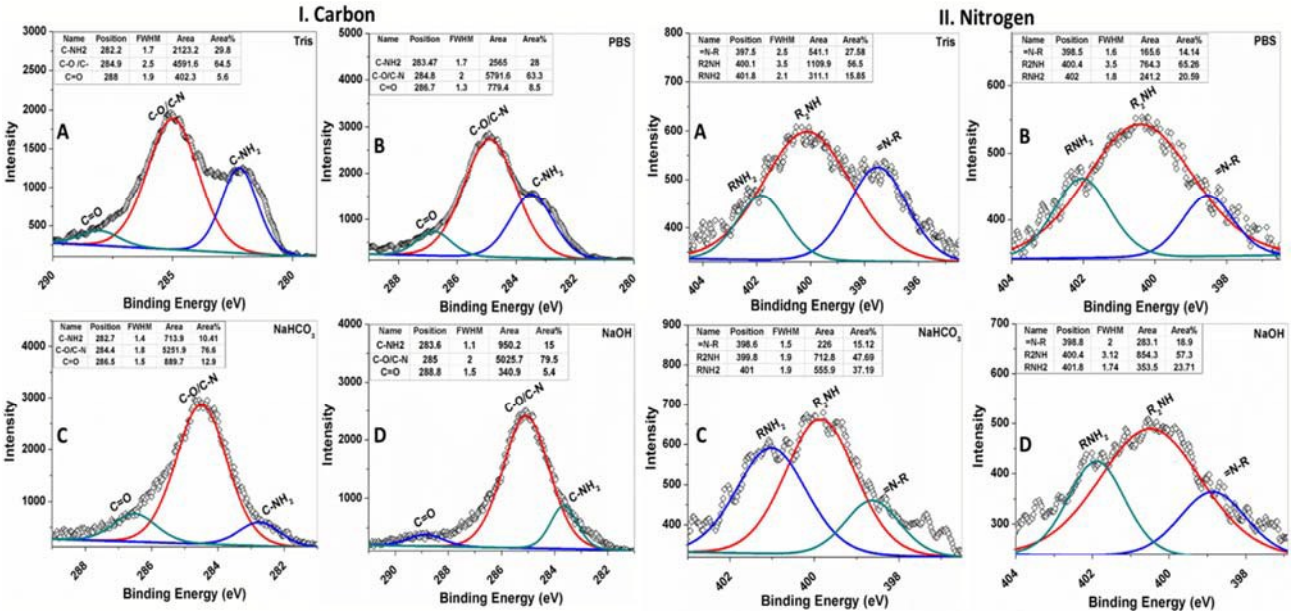

Figure 9: HR-XPS deconvoluted spectra of I. C 1s peaks and II. N 1s peaks of (A) Tris-PDA, (B) PBS-PDA, (C) NaHC – PDA and (D) NaOH-PDA prepared on PET films.

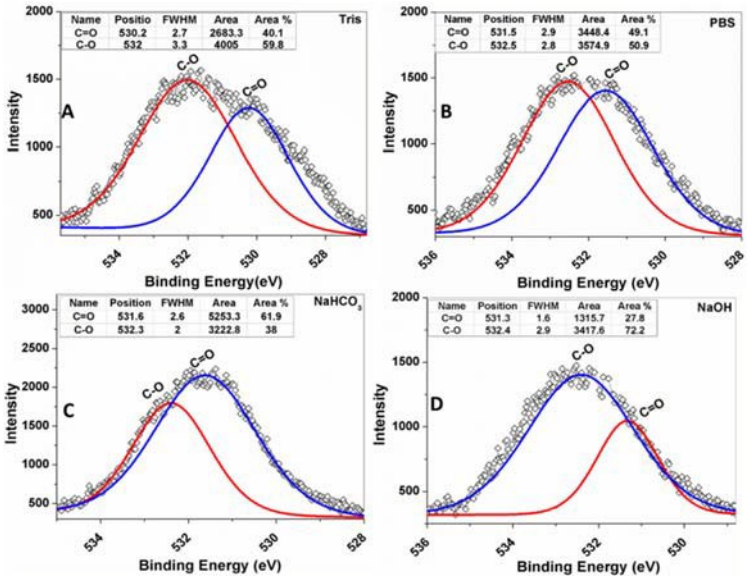

Figure 10: Deconvoluted O1s XPS spectra of the PDA coated PET films prepared in different solvents; (A) Tris-PDA, (B) PBS-PDA, (C) NaHC – PDA and (D) NaOH-PDA prepared on PET films.

The XPS deconvoluted O1s spectra (Fig. 10) supports the fact that Tris and OH (from NaOH) decreases the percentage of C=O in Tris-PDA and NaOH-PDA coatings on account of their covalent incorporation in to PDA layers thus minimizing contribution of Quinone moieties. The O1s deconvolution shows two peak indicating the presence of C=O and C-O group respectively (Fig. 10). The area analysis of deconvoluted peaks as shown in inset tables of Fig. 10 reveals that Tris-PDA and NaOH-PDA contains the lower amount of C=O while the $NaHCO_3$ contains higher percentage of same. It's worth to note that C-O percentage was highest for Na-PDA followed by Tris-PDA which was because of covalent binding of OH (from NaOH) and NH_2 group (from Tris) to the C=O of the quinones thus converting C=O to C-O groups. Furthermore, C=O percentage was least (27 %) in the Na-PDA which can be explained on basis of stronger nucleophilicity of –OH group compared to -NH_2 of Tris. All these analysis thus clearly reveals and supports the different chemical composition/constitutions of PDA coatings which were controlled by the specific polymerisation solvent.

View Article Online
DOI: 10.1039/C7CP08406D
ARTICLE Journal Name

Effect of different PDA coatings on Antibacterial activity

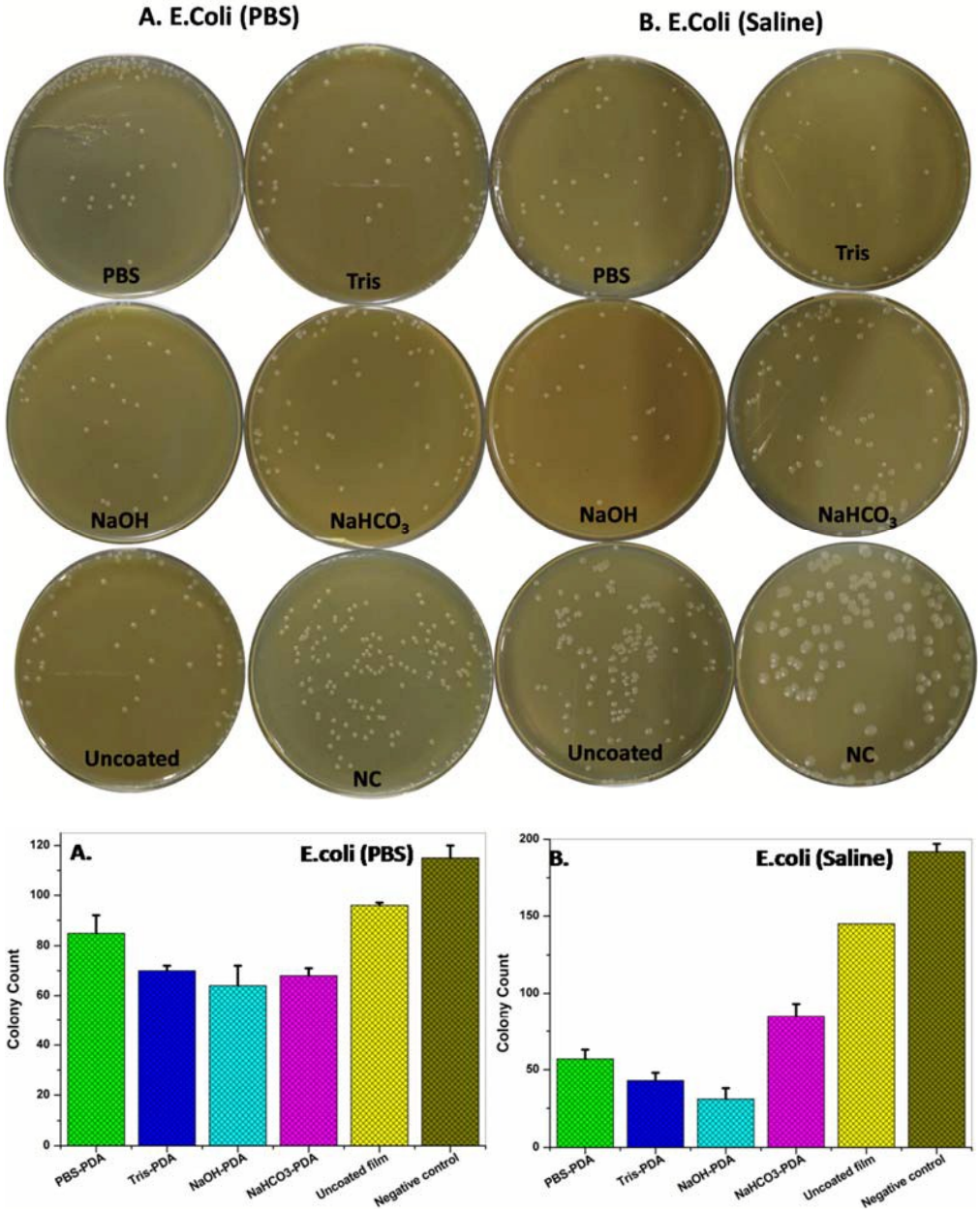

Figure 11: Culture plate Images showing colonies of E.*coli* on an Agar plate in PBS and Saline medium with corresponding bar graphs showing colony counts of the plates. All experiments were performed in triplicate.

View Article Online
DOI: 10.1039/C7CP08406D

Journal Name

ARTICLE

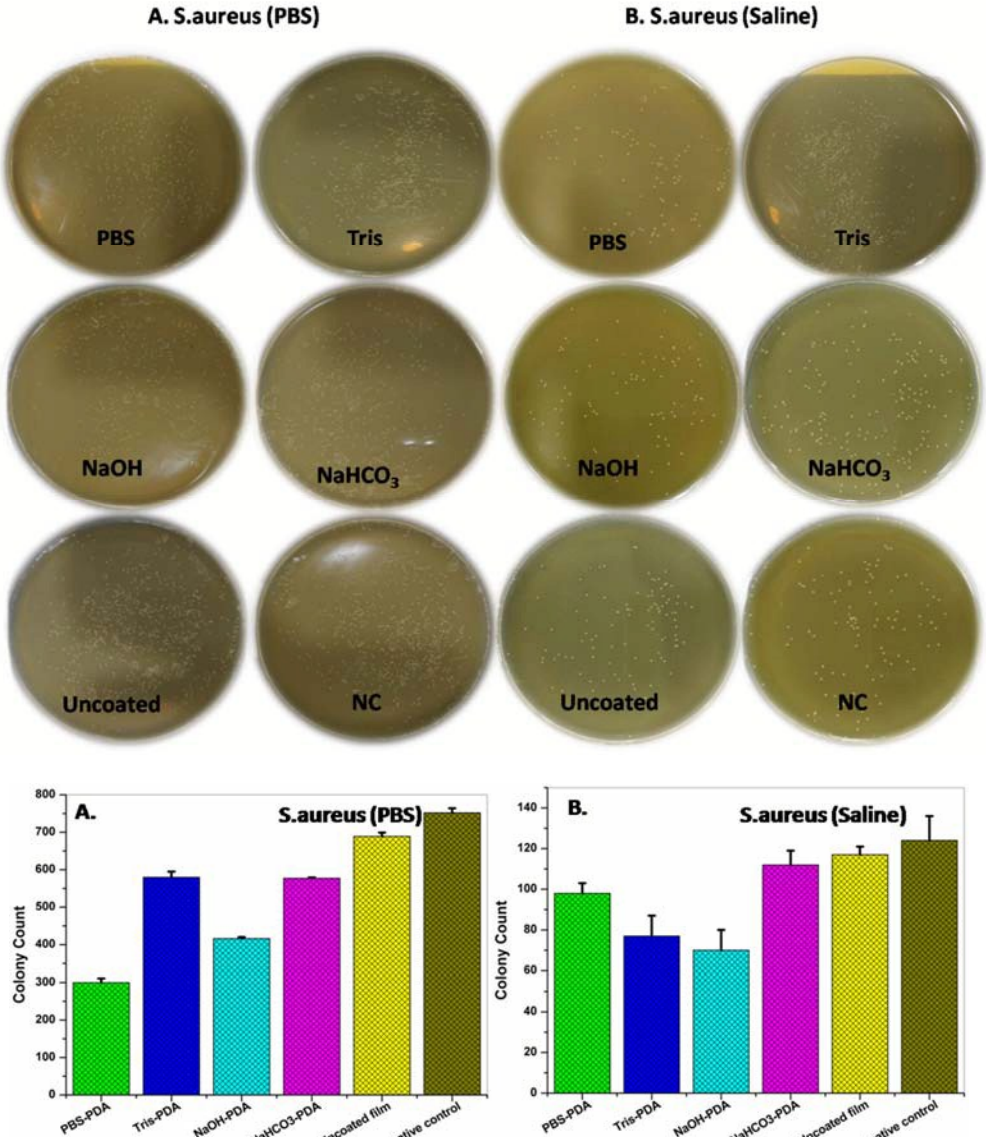

Figure 12: Culture plate Images showing colonies of S.*aureus* on an Agar plate in PBS and Saline medium with corresponding bar graphs showing colony counts of the plates. All experiments were performed in triplicate.

For antibacterial studies two bacterial strains, gram negative E.*coli* and gram positive S*. aureus were* selected*.* The antibacterial activity was evaluated using decrease in colony formation method after incubation with the PDA films. The representative optical images and culture count for E.coli and S.aureus showing number of bacterial colonies counted manually after 60 minutes of incubation with PDA films is shown in Fig.11 and Fig. 12 respectively.

It was observed that for the antibacterial studies carried out in PBS and saline medium, the NaOH-PDA shows highest antibacterial activity followed by Tris-PDA as directly evidenced from reduction in number of bacterial colonies. It can be suggested that E.coli being negatively charged is strongly repelled by the presence of nucleophilic –OH groups on the surface of PDA layers prepared in Tris and NaOH solvents. Compared to the PBS, saline medium

View Article Online
DOI: 10.1039/C7CP08406D

shows higher antibacterial activity for the tested PDA layers. The difference in antibacterial activity was much significant for Tris-PDA and NaOH-PDA layers.

In addition to the manual colony counting method the reduction in cfu/mL were also obtained by OD calculation method after treatment of the PDA films with respective culture and is shown in Fig. 13.Both the methods for evaluating antibacterial activities; manual colony counting and OD measurement methods were in agreement showing similar antibacterial activity trend.

For the gram positive bacteria S.*aureus* also, the antibacterial activity were found to be much higher in saline compared to PBS medium. Similarly, Tris-NaOH and NaOH-PDA shows higher antibacterial activities against S.aureus in saline. However in case of S.*aureus* an exception was found for Tris-PDA which shows lower antibacterial activity in PBS medium compared to other PDA layers. Nevertheless, the antibacterial activities were found to be higher for NaOH-PDA and Tris-PDA, which were attributed to the increase in the surface hydroxyl groups, contributed by covalent incorporation of nucleophilic Tris and NaOH in to PDA layers.

Thus, it can be conclusively shown that the PDA-coated PET films show significant antibacterial activity compared to native PET films. Among E.*coli* and S.*aureus,* the antibacterial activities of all PDA layers were significantly higher towards the gram negative bacteria E.*coli*.

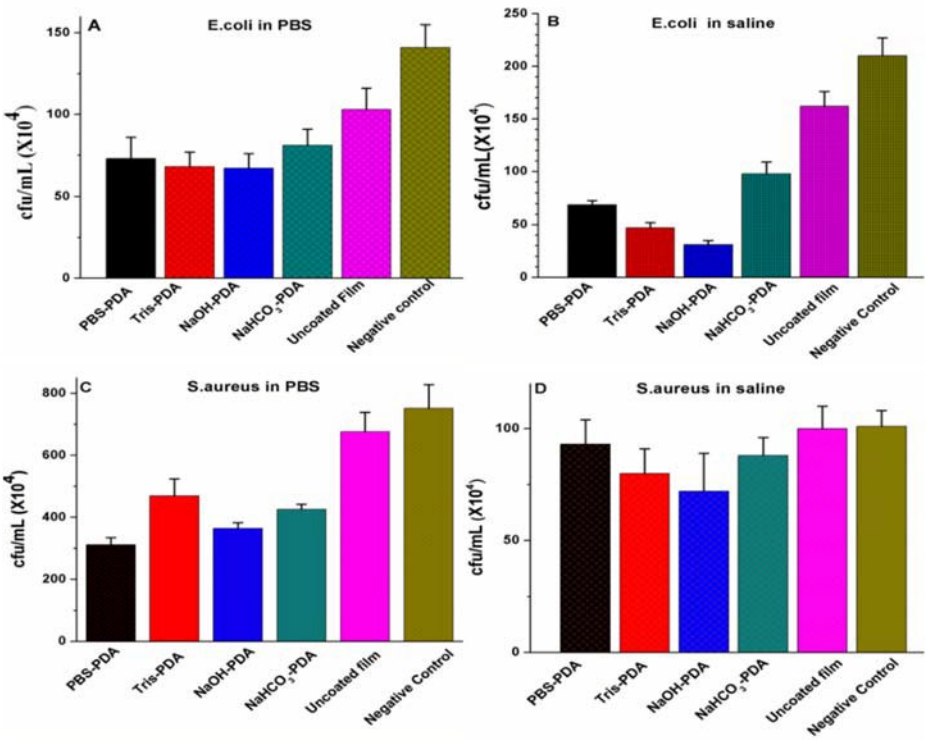

Figure 13: Bar graph showing the CFU obtained after treatment of different PDA coated films with bacterial strain in PBS and Saline medium for; (A&B)- E.coli bacteria and (C&D)- S. aureus bacteria. All experiments were performed in triplicate.

Although, more studies will be required to understand the exact mechanism of enhanced antibacterial behaviour of Tris-PDA and NaOH-PDA compared to PBS-PDA and NaHCO3-PDA nevertheless, it can be safely proposed on the basis of available experimental evidences that covalent binding of the Tris and NaOH solvent to PDA layers is responsible for enhanced antibacterial properties.

Materials and Methods

Chemical and Reagents

Sodium hydroxide (NaOH), Sodium bicarbonate ($NaHCO_3$), Sodium Chloride (NaCl), Potassium Chloride (KCl), Sodium Hydrogen Phosphate (Na_2HPO_4), Potassium Dihydrogen Phosphate (KH_2PO_4) and other chemicals were purchased from Finar (India). Dopamine hydrochloride was obtained from Sigma Aldrich, (St. Louis, MO, USA). Tris buffer was purchased from Rankem, India and PET sheets obtained from Sumilion Polyester Ltd. All the experiments were carried out in deionised water.

Coating of Polydopamine layers on the PET surfaces

The PET sheets (20 x 10 mm) were washed by ultrasonication in DI water and ethanol for 15 minutes each. Thereafter, the PET sheets were rinsed with DI water and immersed in to the glass vial containing polydopamine solution, 2 mg/mL in 10 mM buffer solution. The final pH of the buffers were adjusted to the pH = 8.5. The vials containing immersed PET films were allowed to shake on

View Article Online
DOI: 10.1039/C7CP08406D

rotary shaker in air for different time intervals at room temperature.

After designated time, the PDA coated PET films were taken out from the vials and washed with the corresponding fresh buffer solutions. Thereafter, the PDA coated surfaces were rinsed with copious amount of DI water and finally with ethanol. The films were dried under nitrogen stream and stored at 4˚C in dark before characterization.

Antibacterial studies

Antibacterial studies were done using the decrease in colony formation unit method. Bacterial cultures of E.*coli* and S. *aureus* was inoculated in the LB broth and incubated at 37 ^{0}C for 24 hours. After 24 hours of incubation cultures were centrifuged at 10000 RPM at 4˚C. The pellet was washed with sterile PBS for four times and diluted to get 10^5 CFU/ ml. (at OD_{600}) using PBS (pH=7.4). 100 µL of diluted culture was then added to the thin film in sterile eppendorf tube and incubated it at 37˚C for 60mins in dark. After that treated films were washed with sterile PBS to collect bacterial cells from the films and diluted to 10^3 CFU/ ml with sterile PBS. 100 µL of this diluted cells was spreaded on the LB agar plates and incubated at 37˚C for 24 hours. Similar study was performed using Saline also to check the antibacterial activity in PBS and saline. Manual colony counting's were also done to supplement the cfu data obtained by OD method.

Characterisation

Contact Angle was measured using OCA 20 instrument (Data physics Products, Filderstadt, Germany) with water droplet size of 0.3 µL. For each sample, SCA 20 software was used to extract contact angle. All the measurements were done at least three times at room temperature on both the sides of the films. SCA 20 software was used for the quantification of contact angle.

Attenuated Total Reflectance Fourier Transform Infrared (ATR-FTIR) was done using a Shimadzu Infinity1S-Wl spectrophotometer at resolution of 4cm^{-1} in the wavenumber range of 500-4000 cm^{-1} and scan rate of 150 scans per minute.

X-ray photoelectron spectroscopy was performed using micron ESCA (Electron Spectroscopy for Chemical Analysis) from Oxford Instrument, (Germany).

Atomic force measurements were performed on Bruker Multimode-8.

FEG-SEM was done using JEOL JSM-7600F along with EDS.

Conclusions

In conclusion we have successfully shown that buffers used in polymerisation of dopamine to polydopamine influences the morphological features of PDA coatings on PET films. The morphological and chemical features were well supported by FEG-SEM, AFM, XPS and ATR-FTIR and contact angle measurements. The different coatings prepared in different buffers like PBS, Tris, NaOH and $NaHCO_3$ shows distinct morphological features ranging from particles to patches formed on surface of PET. The chemical composition as revealed by XPS analysis confirms that the choice of buffer controls the percentage of the particular functional group present in PDA coatings. The different morphologies of PDA coatings show different antibacterial properties as evaluated using zone of inhibition method. The PDA coatings prepared in Tris buffer shows maximum and significant antibacterial properties compared to the other buffers which may be attributed to the presence of –CH_2-OH groups upon incorporation of Tris in to the PDA coatings.

These findings will provide a way head to design surfaces with controllable morphology and chemistry for applications with controlled antibacterial activities. In addition the study provides an efficient insight in to the surfaces controlled antibacterial phenomenon which will help in designing more potent antibiofouling surfaces in particular and other articles of human use in general. The finding also indicates that PET films coated with PDA using different buffers can help in designing potent antibacterial PET surfaces thus increasing the shelf life of articles of common use having PET constituents.

Conflicts of interest

There are no conflicts to declare.

Acknowledgements

This work was supported by a grant from the SVNIT, Surat (Fellowship to NS) and DST (YSS/2015/001184) (Fellowship to KP) and financial support for the project. We would like to acknowledge MNIT Jaipur for providing us AFM and XPS, and SAIF IIT Bombay for FEG SEM. We also like to thank Department of Biotechnology, Himachal Pradesh University.

Notes and references

1. S. Dürr and J. C. Thomason, *Biofouling*, Wiley, 2009.
2. H. C. Flemming, *Applied microbiology and biotechnology*, 2002, 59, 629-640.
3. V. B. Damodaran and N. S. Murthy, *Biomaterials Research*, 2016, 20, 18.
4. J. Gallo, M. Holinka and C. S. Moucha, *International Journal of Molecular Sciences*, 2014, 15, 13849-13880.
5. M. M. Williams, C. R. Armbruster and M. J. Arduino, *Biofouling*, 2013, 29, 147-162.
6. I. Banerjee, R. C. Pangule and R. S. Kane, *Advanced materials (Deerfield Beach, Fla.)*, 2011, 23, 690-718.
7. H. A. Patel, Google Patents, 2012.
8. G. Müller, H. Benkhai, R. Matthes, B. Finke, W. Friedrichs, N. Geist, W. Langel and A. Kramer, *Biomaterials*, 2014, 35, 5261-5277.
9. J. Hasan, R. J. Crawford and E. P. Ivanova, *Trends in biotechnology*, 2013, 31, 295-304.

View Article Online
DOI: 10.1039/C7CP08406D

10. C. Zhao, L. Li, Q. Wang, Q. Yu and J. Zheng, *Langmuir*, 2011, 27, 4906-4913.
11. S. H. Ku, J. S. Lee and C. B. Park, *Langmuir*, 2010, 26, 15104-15108.
12. H. Lee, B. P. Lee and P. B. Messersmith, *Nature*, 2007, 448, 338-341.
13. X. Chen, Y. Huang, G. Yang, J. Li, T. Wang, O. H. Schulz and L. K. Jennings, *Curr Pharm Des*, 2015, 21, 4262-4275.
14. Y. Liu, K. Ai and L. Lu, *Chem Rev*, 2014, 114, 5057-5115.
15. H. Lee, S. M. Dellatore, W. M. Miller and P. B. Messersmith, *Science (New York, N.Y.)*, 2007, 318, 426-430.
16. L. Su, Y. Yu, Y. Zhao, F. Liang and X. Zhang, *Sci Rep*, 2016, 6, 24420.
17. C. C. Ho and S. J. Ding, *J Biomed Nanotechnol*, 2014, 10, 3063-3084.
18. J. L. Dalsin, B. H. Hu, B. P. Lee and P. B. Messersmith, *J Am Chem Soc*, 2003, 125, 4253-4258.
19. D. E. Fullenkamp, J. G. Rivera, Y. K. Gong, K. H. Lau, L. He, R. Varshney and P. B. Messersmith, *Biomaterials*, 2012, 33, 3783-3791.
20. J. Jiang, L. Zhu, L. Zhu, H. Zhang, B. Zhu and Y. Xu, *ACS Appl Mater Interfaces*, 2013, 5, 12895-12904.
21. T. S. Sileika, H. D. Kim, P. Maniak and P. B. Messersmith, *ACS Appl Mater Interfaces*, 2011, 3, 4602-4610.
22. C. Zhang, H. N. Li, Y. Du, M. Q. Ma and Z. K. Xu, *Langmuir*, 2017, 33, 1210-1216.
23. K. Dumri and D. Hung Anh, *Enzyme Res*, 2014, 2014, 389739.
24. Z. Lu, J. Xiao, Y. Wang and M. Meng, *J Colloid Interface Sci*, 2015, 452, 8-14.
25. Z. Yang, Y. Wu, J. Wang, B. Cao and C. Y. Tang, *Environ Sci Technol*, 2016, 50, 9543-9550.
26. K. Dumri and D. Hung Anh, *Enzyme research*, 2014, 2014.
27. N. Mohd Daud, I. F. Saeful Bahri, N. A. Nik Malek, H. Hermawan and S. Saidin, *Colloids Surf B Biointerfaces*, 2016, 145, 130-139.
28. M. C. Sin, Y. M. Sun and Y. Chang, *ACS Appl Mater Interfaces*, 2014, 6, 861-873.
29. X. Sun, L. Cheng, J. Zhao, R. Jin, B. Sun, Y. Shi, L. Zhang, Y. Zhang and W. Cui, *Journal of Materials Chemistry B*, 2014, 2, 3636-3645.
30. X. Liu, J. Cao, H. Li, J. Li, Q. Jin, K. Ren and J. Ji, *ACS Nano*, 2013, 7, 9384-9395.
31. S. Hong, K. Y. Kim, H. J. Wook, S. Y. Park, K. D. Lee, D. Y. Lee and H. Lee, *Nanomedicine*, 2011, 6, 793-801.
32. J. Liebscher, R. Mrówczyński, H. A. Scheidt, C. Filip, N. D. Hădade, R. Turcu, A. Bende and S. Beck, *Langmuir*, 2013, 29, 10539-10548.
33. D. R. Dreyer, D. J. Miller, B. D. Freeman, D. R. Paul and C. W. Bielawski, *Langmuir*, 2012, 28, 6428-6435.
34. N. F. Della Vecchia, A. Luchini, A. Napolitano, G. D'Errico, G. Vitiello, N. Szekely, M. d'Ischia and L. Paduano, *Langmuir*, 2014, 30, 9811-9818.
35. R. A. Zangmeister, T. A. Morris and M. J. Tarlov, *Langmuir*, 2013, 29, 8619-8628.
36. N. F. Della Vecchia, R. Avolio, M. Alfè, M. E. Errico, A. Napolitano and M. d'Ischia, *Advanced Functional Materials*, 2013, 23, 1331-1340.
37. N. F. Della Vecchia, A. Luchini, A. Napolitano, G. D'Errico, G. Vitiello, N. Szekely, M. d'Ischia and L. Paduano, *Langmuir*, 2014, 30, 9811-9818.
38. K. Bazaka, M. V. Jacob, W. Chrzanowski and K. Ostrikov, *RSC Advances*, 2015, 5, 48739-48759.
39. A. Shirakura, M. Nakaya, Y. Koga, H. Kodama, T. Hasebe and T. Suzuki, *Thin Solid Films*, 2006, 494, 84-91.
40. M. Nakaya, A. Uedono and A. Hotta, *Coatings*, 2015, 5, 987-1001.
41. D. L. Schmidt, R. F. Brady, K. Lam, D. C. Schmidt and M. K. Chaudhury, *Langmuir*, 2004, 20, 2830-2836.
42. J. Cui, Y. Yan, G. K. Such, K. Liang, C. J. Ochs, A. Postma and F. Caruso, *Biomacromolecules*, 2012, 13, 2225-2228.
43. A. E. Contreras, Z. Steiner, J. Miao, R. Kasher and Q. Li, *Environ Sci Technol*, 2011, 45, 6309-6315.
44. R. A. Gittens, L. Scheideler, F. Rupp, S. L. Hyzy, J. Geis-Gerstorfer, Z. Schwartz and B. D. Boyan, *Acta Biomater*, 2014, 10, 2907-2918.
45. F. Rupp, R. A. Gittens, L. Scheideler, A. Marmur, B. D. Boyan, Z. Schwartz and J. Geis-Gerstorfer, *Acta Biomater*, 2014, 10, 2894-2906.
46. E. Korin, N. Froumin and S. Cohen, *ACS Biomaterials Science & Engineering*, 2017, 3, 882-889.
47. M. d'Ischia, A. Napolitano, V. Ball, C. T. Chen and M. J. Buehler, *Acc Chem Res*, 2014, 47, 3541-3550.